

Effect of initiator on styrene emulsion polymerisation stabilised by mixed SDS/NP-40 surfactants

C. S. Chern*, S. Y. Lin, S. C. Chang, J. Y. Lin and Y. F. Lin

Department of Chemical Engineering, National Taiwan Institute of Technology,
 Taipei, 106 Taiwan, Republic of China

(Received 16 June 1997)

This paper deals with the effects of initiator concentration ([I]) on the styrene (STY) emulsion polymerisation stabilised by the mixed anionic/nonionic surfactants, sodium dodecyl sulfate (SDS)/nonylphenol polyethoxylate with an average of 40 ethylene oxides per molecule (NP-40). The reaction system stabilised only by SDS ([NP-40] = 0 wt%) results in an increase in the rate of polymerisation (R_p) with [I]. For the system stabilised only by NP-40 ([NP-40] = 100 wt%), R_p remains relatively constant when [I] increases. For the system with [NP-40] = 50 or 80 wt%, R_p first increases to a maximum and then decreases with increasing [I]. Furthermore, the total scrap, presumably caused by bridging flocculation and/or formation of complex between the ethylene oxide units of NP-40 and the particle surface SO_4^- end-groups derived from the persulfate initiator, first remains relatively constant and then increases rapidly to a maximum with increasing [I]. Beyond the maximum, the total scrap starts to decrease with increasing [I]. Smith–Ewart case II theory (i.e., $n_s = 0.6$ and $n_i = 0.4$ in the relationship $N_p \sim [S]^{n_s} [I]^{n_i}$) is only applicable to the system with [NP-40] = 0 wt%. At [I] = 1.38×10^{-3} M, systems with [NP-40] = 0, 50 and 80 wt% result in comparable latex particle sizes (d_p) and relatively monodisperse size distributions throughout the reaction. On the other hand, the system with [NP-40] = 100 wt% shows the largest d_p and the broadest size distribution, which is attributed to the long particle nucleation period and/or limited flocculation. © 1998 Elsevier Science Ltd. All rights reserved.

(Keywords: emulsion polymerisation; styrene; mixed anionic and nonionic surfactants)

INTRODUCTION

Emulsion polymerisation involves dispersion of a relatively water-insoluble monomer (e.g. styrene, STY) in water at the reaction temperature with the aid of surfactants, followed by addition of the persulfate initiator solution. The resultant latex products are widely used in adhesives, coatings, binders, thermoplastics and in the rubber industries. A latex product is a dispersion of innumerable polymer particles (ca. 50–10 000 nm in diameter) in the aqueous phase. These submicron particles are unstable in nature and they can be stabilised by the electrostatic repulsion force provided by anionic surfactants¹ and/or steric repulsion force provided by nonionic surfactants² to override the van der Waals attraction force between the interactive particles. Anionic surfactants such as sodium dodecyl sulfate $\text{C}_{12}\text{H}_{25}\text{SO}_4\text{Na}^+$ (SDS) serve as strong particle generators^{3,4}, whereas nonionic surfactants such as nonylphenol polyethoxylate with an average of 40 ethylene oxides per molecule $\text{C}_9\text{H}_{19}-\text{C}_6\text{H}_4-\text{O}-(\text{CH}_2\text{CH}_2\text{O})_{40}\text{H}$ (NP-40) provide the latex product with excellent stability toward high electrolyte concentrations, freeze–thaw cycling and high shear rates^{5,6}.

The particle nucleation period is quite short in emulsion polymerisation, but it has a crucial influence on the final latex particle size (d_p) and size distribution. Control of d_p is crucial in determining the quality of latex products. According to the micellar nucleation mechanism (Smith–

Ewart theory)^{7–10}, primary particle nuclei are generated via capture of the relatively hydrophobic oligomeric radicals in the aqueous phase by the monomer-swollen micelles. The number of primary particles nucleated is controlled by the amount of surfactant available for stabilising the generated polymer particle–water interfacial area. The remainder of the reaction is simply the growth of these primary particles via polymerisation of the imbibed monomer provided by the monomer droplet reservoir. The number of latex particles (N_p) produced at the end of polymerisation, as predicted by Smith–Ewart theory, follows the following relationship:

$$N_p \sim [S]^{n_s} [I]^{n_i} \quad (1)$$

where [S] and [I] are the concentrations of surfactant and initiator, respectively. For example, the values of n_s and n_i are equal to 0.6 and 0.4, respectively, for polymerisation systems which follow Smith–Ewart case II theory. This relationship has been confirmed in the STY emulsion polymerisation stabilised only by SDS. However, the literature dealing with the particle nucleation and growth mechanisms for the reaction system stabilised by the mixed SDS/NP-40 surfactants has been scarce.

In our previous report¹¹, the critical micelle concentrations (CMC) in an aqueous solution of the mixed SDS/NP-40 surfactants at both 25 and 80°C were determined by surface tension measurements. It was shown that the CMC of the mixed surfactant solution decreases with an increase in the weight percentage of NP-40 in the surfactant mixture ([NP-40]). Furthermore, the CMC of the mixed surfactant solution at 80°C is slightly higher than that at 25°C and the

* To whom correspondence should be addressed

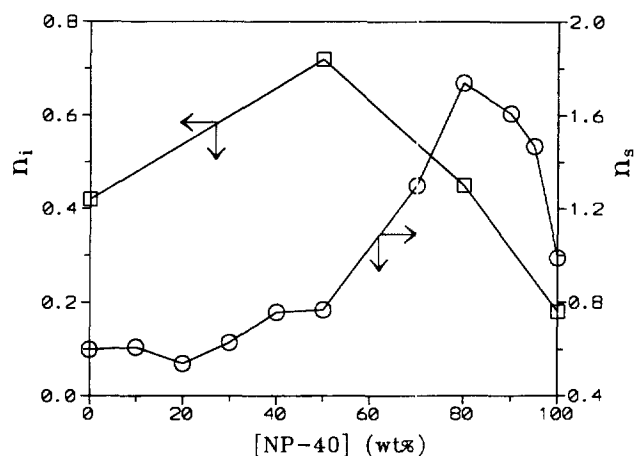


Figure 1 Smith-Ewart parameters n_i and n_s as a function of the weight percentage of NP-40 in the surfactant mixture when $[I]$ is in the range of 5.00×10^{-4} – 6.43×10^{-3} M. □, n_i ; ○, n_s .

difference diminishes when [NP-40] approaches 100 wt%. At a constant mixed surfactant concentration ($[S]$), the number of mixed micelles formed immediately before the start of particle nucleation should be a function of such parameters as [NP-40], the aggregation number of a mixed micelle, polymerisation temperature, etc. These parameters are expected to show a significant influence on N_p , if the micellar nucleation mechanism predominates during the particle nucleation period. Recently, the mixed SDS/NP-40 surfactants were used to examine the generality of Smith-Ewart case II theory in our laboratory¹². The concentration of sodium persulfate ($[I]$) was kept constant in most of the experiments. The $\log N_p$ versus $\log [S]$ data are consistent with Smith-Ewart case II theory (i.e., $n_s = 0.6$) only when [NP-40] is below 30 wt%. Nevertheless, the polymerisation system deviates from Smith-Ewart case II theory significantly ($n_s > 0.6$) when [NP-40] is greater than 50 wt% (see the circular data points in Figure 1). Furthermore, the steric stabilisation effect provided by NP-40 alone is not sufficient to prevent the latex particles from flocculating with one another during polymerisation. As a consequence, the resultant latex particles stabilised only by NP-40 are quite large. On the other hand, the electrosterically stabilised latex particles are relatively stable due to the synergistic stabilisation effects provided by SDS and NP-40 and, therefore, limited flocculation is greatly retarded during polymerisation. Thus, the final latex particle size for the system stabilised by SDS/NP-40 is generally smaller.

The objective of this work was to gain a better understanding of the role of the persulfate initiator in the STY emulsion polymerisation stabilised by the mixed SDS/NP-40 surfactants. The values of n_i as a function of [NP-40] were determined to further assess the applicability of Smith-Ewart case II theory (see equation (1)). Furthermore, the concentration of sodium ions derived from the persulfate initiator increases with increasing $[I]$. The increased ionic strength of the aqueous solution provided by the counter-ion Na^+ tends to destabilise the latex particles and, thereby, increases the probability of forming large flocs (scrap) during polymerisation. Thus, it is interesting to study the effectiveness of the mixed SDS/NP-40 surfactants in stabilising the latex particles in the course of polymerisation, especially when $[I]$ is high.

EXPERIMENTAL

Materials

The chemicals used in this work include styrene (Taiwan Styrene Monomer Co.), sodium dodecyl sulfate (Henkel Co.), nonylphenol polyethoxylate with an average of 40 ethylene oxides per molecule (Union Carbide), sodium persulfate (Reidel-de-Haen), sodium sulfate (Ishizu Pharmaceutical Co.), nitrogen (Ching-Feng-Harg Co.), and deionised water (Barnstead NANOpure water purification system, specific conductance $< 0.057 \mu\text{S cm}^{-1}$). The monomer STY was distilled under reduced pressure before use. All other chemicals were used as received.

Polymerisation process

Batch emulsion polymerisation was carried out in a baffled glass reactor equipped with a four-bladed fan turbine agitator, a thermometer, and a reflux condenser (reactor volume 1.5 l). A typical recipe is shown in Table 1. The parameter $[S]$ was kept constant at 6×10^{-3} M throughout this work, whereas $[I]$ was varied from 5.02×10^{-4} to 9.20×10^{-2} M. This value of $[S]$ is about 1.5 times the CMC (80°C) of the SDS solution and it is always higher than the CMCs (80°C) of the mixed surfactant solutions with various levels of [NP-40]¹¹. The total solid content was designed at 15%. First, water, SDS/NP-40, and STY were charged to the reactor and the reactor charge was purged with nitrogen for 10 min to remove dissolved oxygen while heating to 80°C , followed by addition of the initiator solution. The polymerisation was carried out at 80°C over a period of 4 h. The agitation speed was maintained at 400 rev min^{-1} throughout the reaction.

Characterisation of latex samples

The latex product was filtered through 40-mesh (0.42 mm) and 200-mesh (0.074 mm) screens in series to collect the filterable solids. Scraps adhering to the agitator, thermometer, and reactor wall were also collected. The total scrap data reported in this work represents the large flocs collected by the 40- and 200-mesh screens in series plus those adhering to the agitator, thermometer, and reactor wall. The total solid content of the latex sample was determined by the gravimetric method.

Particle size (d_p) data were obtained from the dynamic light scattering (DLS) method (Otsuka, Photal LPA-3000/3100). If necessary, the turbid latex sample comprising large particles produced at a relatively high monomer conversion was further diluted with deionised water to adjust the CPS value to the range 8000–12 000. The parameter 'accumulation times' was set at 50 throughout this study. The d_p data reported in this work represent an average of at least three measurements and these data show an error of 4% or less. Some latex samples taken from a series of experiments with $[S] = 6 \times 10^{-3}$ M, $[I] = 1.38 \times 10^{-3}$ M, various levels of

Table 1 A typical recipe for the batch emulsion polymerisation of styrene: $[S] = 6 \times 10^{-3}$ M, [NP-40] = 50 wt%, $[I] = 1.38 \times 10^{-3}$ M

	Reagent	Weight (g)
Reactor charge	H ₂ O	764.91
	SDS	1.155
	NP-40	1.155
	STY	134.99
Initiator solution	H ₂ O	5
	Na ₂ S ₂ O ₈	0.252

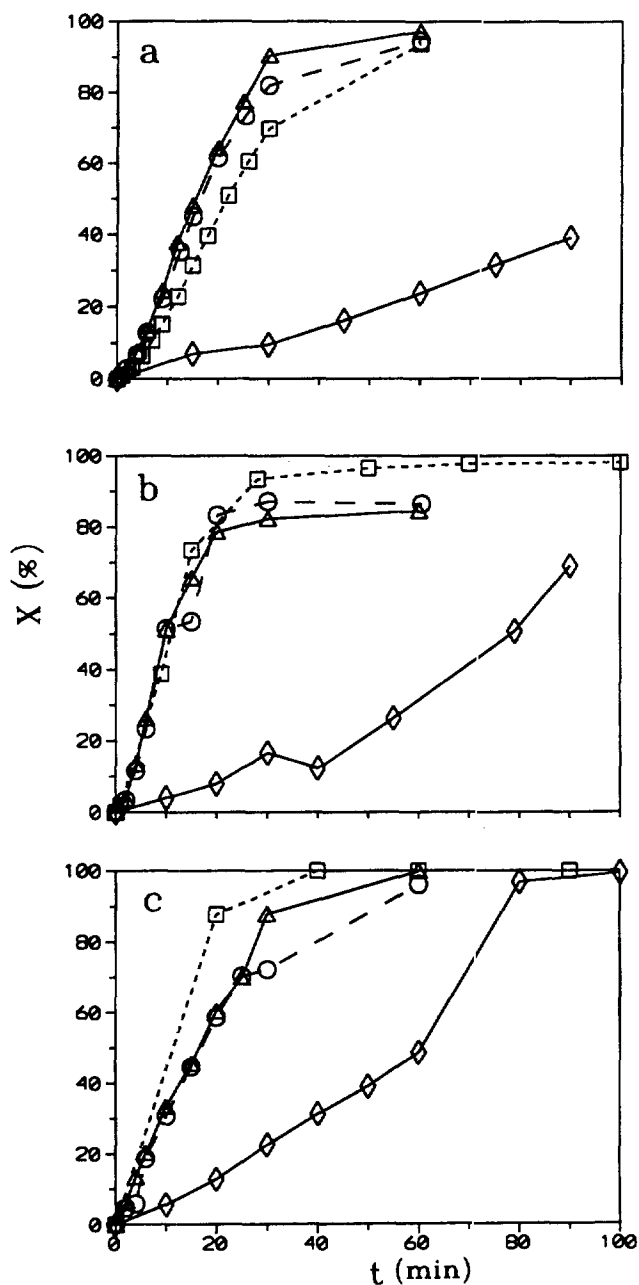


Figure 2 Representative monomer conversion versus reaction time profiles: (a) $[I] = 0.00138 \text{ M}$; (b) $[I] = 0.0105 \text{ M}$; (c) $[I] = 0.0493 \text{ M}$.

[NP-40] (0, 50, 80 and 100 wt%) and various monomer conversions (ca. 23, 50 and 95%) were chosen for further examination by transmission electron microscopy (TEM) (JEOL JSM-1200EXII). Approximately 500 particles were measured for each latex sample.

RESULTS AND DISCUSSION

Reaction kinetics

Representative monomer conversion (X) versus reaction time (t) profiles with $[I] = 1.38 \times 10^{-3}$, 1.05×10^{-2} and $4.93 \times 10^{-2} \text{ M}$ are shown in Figure 2a, b and c, respectively. When $[I]$ is below $1.05 \times 10^{-2} \text{ M}$, the rate of change in X with t (dX/dt , obtained from the least-squares best-fitted slope of the linear portion of the X versus t curve in Figure 2a, which is proportional to the rate of polymerisation) in decreasing order is: [NP-40] = 80 wt% ~ [NP-40] = 50 wt% > [NP-40] = 0 wt% \gg [NP-40] = 100 wt%. This trend is consistent with the work of Chern *et al.*¹² However, the dX/dt data in decreasing order become: [NP-40] = 0 wt% > [NP-40] = 80 wt% ~ [NP-40] = 50 wt% \gg [NP-40] = 100 wt% when $[I]$ is above $1.05 \times 10^{-2} \text{ M}$ (see Figure 2c). This transition occurs at $[I] = 1.05 \times 10^{-2} \text{ M}$, in which the dX/dt data in decreasing order are: [NP-40] = 0 wt% ~ [NP-40] = 80 wt% ~ [NP-40] = 50 wt% \gg [NP-40] = 100 wt% (see Figure 2b).

The $\log N_p$ versus $\log [I]$ plots for the STY emulsion polymerisation with various levels of [NP-40] are shown in Figure 3. The number of latex particles per litre of water (N_p) shown in this plot was determined by the DLS method. When $[I]$ is in the range of 5.0×10^{-4} to $6.4 \times 10^{-3} \text{ M}$, the slopes of the $\log N_p$ versus $\log [I]$ data (i.e. n_i shown in equation (1)) are all positive for the experiments with [NP-40] = 0, 50, 80 and 100 wt% (see Figure 3) when $[I]$ is in the range 6.4×10^{-3} to $4.9 \times 10^{-2} \text{ M}$, the values of n_i are also positive for the reactions with [NP-40] = 0 and 100 wt% (see the square and diamond data points in Figure 3). However, the parameter n_i becomes negative for the reaction with [NP-40] = 50 or 80 wt% (see the circular and triangular data points in Figure 3). Figure 1 shows the calculated n_i as a function of [NP-40] when $[I]$ is within 5.0×10^{-4} to $6.4 \times 10^{-3} \text{ M}$. The parameter n_i was determined by the slope of the least-squares best-fitted $\log N_p$ versus $\log [I]$ straight line. Also included in Figure 1 are the n_s versus [NP-40] data taken from Ref.¹². The parameter n_i first increases from 0.42 to a maximum of 0.72, followed by a rapid decrease when [NP-40] increases. These data for n_s and n_i clearly show that Smith-Ewart case II theory is

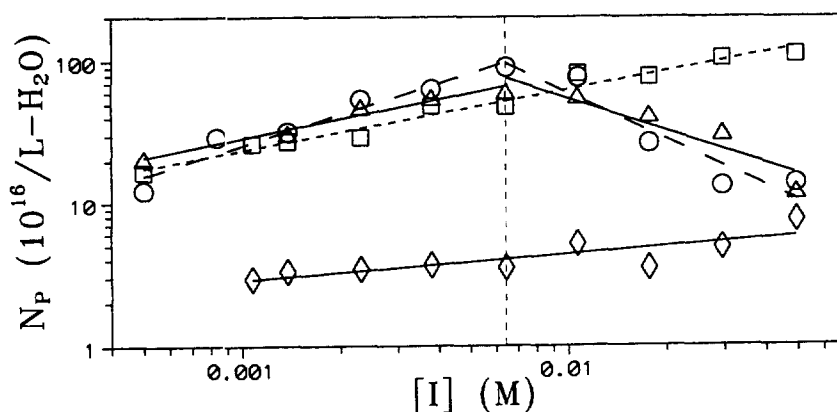


Figure 3 Number of latex particles per litre of water as a function of the concentration of initiator. [NP-40] (wt%): \square , 0; \circ , 50; \triangle , 80; \diamond , 100

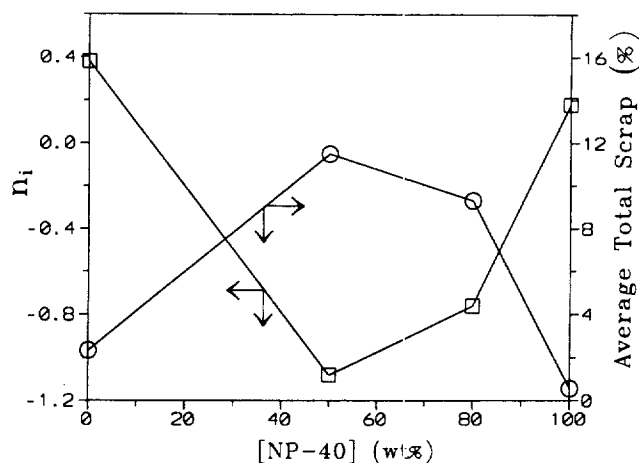


Figure 4 Smith-Ewart parameter n_i and average total scrap as a function of the weight percentage of NP-40 in the surfactant mixture when $[I]$ is in the range of 6.43×10^{-3} – 4.94×10^{-2} M. \square , n_i ; \circ , average total scrap

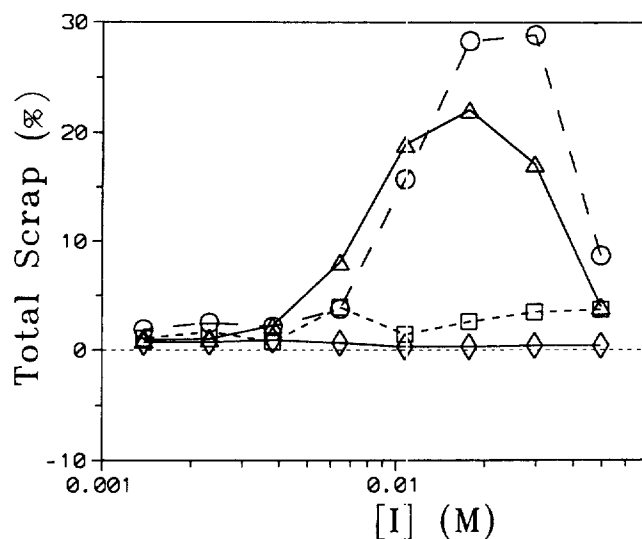


Figure 5 Total scrap as a function of the concentration of initiator. [NP-40] (wt%): \square , 0; \circ , 50; \triangle , 80; \diamond , 100

only valid for the STY emulsion polymerisation with $[\text{NP-40}] = 0$ wt%. The parameter N_p for the polymerisation system stabilised only by NP-40 is rather insensitive to changes in $[I]$ because of the very small value of n_i (0.18). Thus, the parameter $[I]$ is not as effective as $[S]$ in controlling N_p (or d_p) for the system with $[\text{NP-40}] = 100$ wt%.

The square data points in *Figure 4* represent the calculated n_i values as a function of $[\text{NP-40}]$ for $[I]$ values in the range 6.4×10^{-3} to 4.9×10^{-2} M. The circular data points in this plot are the average total scrap data (based on monomer weight) over the same range of $[I]$. The latex stability reflects in the amount of coagulum formed during polymerisation. For the system with $[\text{NP-40}] = 0$ or 100 wt%, the average total scrap is about 2% or less, which is much lower than that (ca. 10%) for the system with $[\text{NP-40}] = 50$ or 80 wt%. Thus, the values of n_i for the relatively stable systems with $[\text{NP-40}] = 0$ and 100 wt% are 0.42 and 0.18, respectively. At relatively high levels of $[I]$, the system with $[\text{NP-40}] = 0$ wt% still follows Smith-Ewart case II theory. On the other hand, the values of n_i for the very unstable systems with $[\text{NP-40}] = 50$ and 80 wt% are

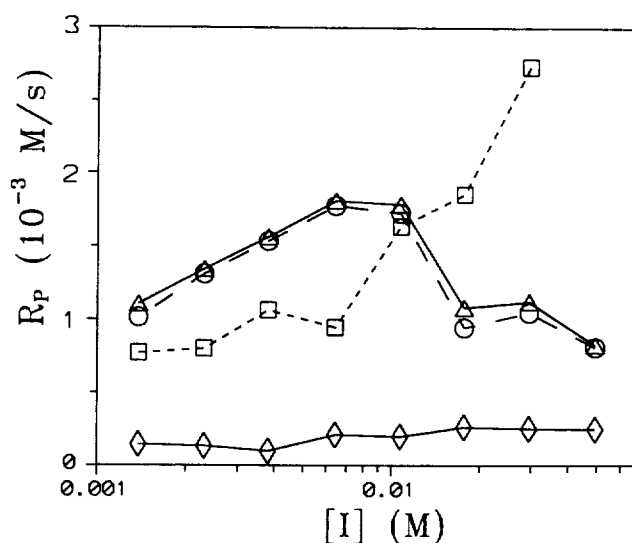


Figure 6 Rate of polymerisation as a function of the concentration of initiator. [NP-40] (wt%): \square , 0; \circ , 50; \triangle , 80; \diamond , 100

–1.08 and –0.76, respectively. These values of n_i represent the condition that N_p decreases rapidly with increasing $[I]$ due to the conversion of the extremely unstable latex particles into large flocs. *Figure 5* shows the total scrap versus $[I]$ data for the systems with various levels of $[\text{NP-40}]$. The total scrap data show that the recipes only containing SDS or NP-40 are quite stable over a wide range of $[I]$. For the recipe containing SDS/NP-40 (50/50 or 20/80), the total scrap first remains relatively constant (ca. 2%) when $[I]$ increases from 1.4×10^{-3} to 3.8×10^{-3} M. The total scrap then increases rapidly to a maximum (ca. 25%) when $[I]$ increases from 3.8×10^{-3} to 1.8×10^{-2} M. This is followed by a rapid decrease in total scrap with $[I]$ being increased from 1.8×10^{-2} to 4.9×10^{-2} M.

The rate of polymerisation (R_p) for emulsion polymerisation can be calculated according to the following equation:

$$R_p = [M]_0 dX/dt = K_p [M]_p (\bar{n} N_p / N_a) \quad (2)$$

where K_p is the propagation rate constant, $[M]_p$ is the concentration of monomer in the particles, \bar{n} is the average number of free radicals per particle and N_a is Avogadro's number. Equation (2) predicts that R_p is proportional to N_p (the number of reaction loci) and \bar{n} . This equation can be used to calculate \bar{n} if the parameters R_p , K_p , $[M]_p$ and N_p are known. During Smith-Ewart Interval II (X is approximately in the range 15–45% for the STY emulsion polymerisation)¹⁴, R_p remains relatively constant due to the steady values of $[M]_p$, \bar{n} and N_p . The parameter R_p can be calculated according to equation (2) (i.e., $R_p = [M]_0 dX/dt$), in which dX/dt is simply the slope of the least-squares best-fitted X versus t straight line during Interval II. The calculated R_p and \bar{n} as a function of $[I]$ are shown in *Figures 6 and 7*, respectively.

Figure 6 shows that R_p increases with increasing $[I]$ for the system stabilised only by SDS because of the increased number of reaction loci (N_p) (see the square data points in *Figure 3*). For the system stabilised only by NP-40, however, R_p remains relatively constant when $[I]$ increases. This is simply due to the fact that N_p increases very slowly with increasing $[I]$ (see the diamond data points in *Figure 3*). As to the system with $[\text{NP-40}] = 50$ or 80 wt%, R_p first increases to a maximum at $[I] \sim 6.4 \times 10^{-3}$ M and thereafter starts to decrease when $[I]$ increases. The corresponding log

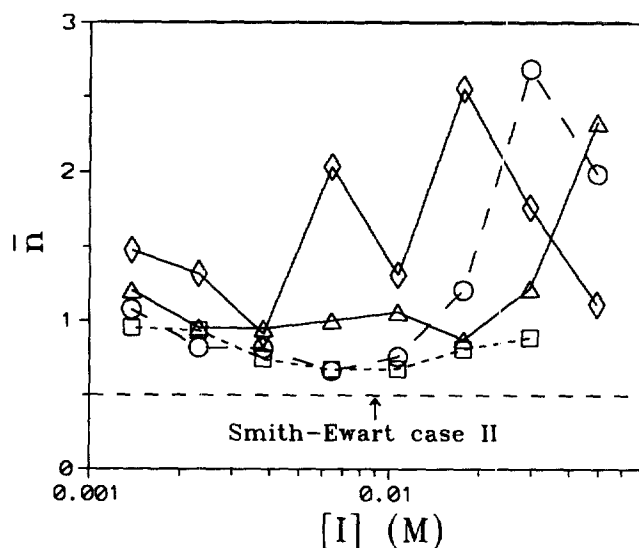


Figure 7 Average number of free radicals per particle as a function of the concentration of initiator. [NP-40] (wt%): □, 0; ○, 50; △, 80; ◇, 100

N_p versus $\log [I]$ plots support this kind of behaviour, as shown by the circular or triangular data points in Figure 3. The slower R_p for the system stabilised only by NP-40 is due to the smaller N_p and/or the more intensive limited flocculation occurring during the particle growth period. Such a limited flocculation process involves the extremely large polymer particle–water interfacial area generated during the particle nucleation period due to the quite low CMC of NP-40 (1.52×10^{-4} M at 80°C)¹¹. Thus, the particle surface coverage of NP-40 may not be high enough to provide the interactive particles with adequate steric stabilisation. These latex particles may thus grow in size by mild aggregation of a few particles. This will result in a reduction in the number of latex particles (or a reduction in the particle–water interfacial area) and, thereby, enhance the particle surface coverage of NP-40. Such a limited flocculation process will cease when the concentration of NP-40 adsorbed on the particle surface increases to a critical level and most of the aggregated particles still be stably dispersed in the aqueous phase. This result is consistent with Refs. 3–17.

Figure 7 shows that all the polymerisations conducted in this work follow Smith–Ewart case III kinetics (i.e., $\bar{n} > 0.5$)⁸. Only when $[I]$ is within 6.4×10^{-3} – 1.1×10^{-2} M, the systems with [NP-40] = 0 and 50 wt% approach Smith–Ewart case II kinetics (i.e., $\bar{n} = 0.5$)⁸. For the system with [NP-40] = 0 wt%, \bar{n} does not change very much (0.81 ± 0.14) over the range of $[I]$ investigated in this work (see the square data points in Figure 7). For the system with [NP-40] = 50 or 80 wt%, \bar{n} first remains relatively constant (0.83 ± 0.25 or 1.04 ± 0.17) up to $[I] \sim 1.1 \times 10^{-2}$ M and then increases significantly with increasing $[I]$ (see the circular or triangular data points in Figure 7). For the system with [NP-40] = 100 wt%, the data of \bar{n} as a function of $[I]$ are quite scattered (within 0.91–2.56), as shown by the diamond data points in Figure 7. The reason for this observation is not clear at this time, but it is probably related to the periodic events of limited flocculation and particle nucleation taking place during polymerisation.

For emulsion polymerisations stabilised only by SDS or NP-40, the number of micelles (N_m) formed immediately before the start of reaction can be estimated by the following

Table 2 Kinetic parameters for batch emulsion polymerisation of styrene at 80°C

Parameter	Numeric value	Units	References
f	1		This work
K_d	1.10×10^{-4}	s^{-1}	18
K_p	342	$\text{M}^{-1} \text{s}^{-1}$	13
$[M]_0$	1.697	M	This work
$[M]_p$	5.2	M	15
m (SDS)	71		19,20
m (NP-40)	8		21

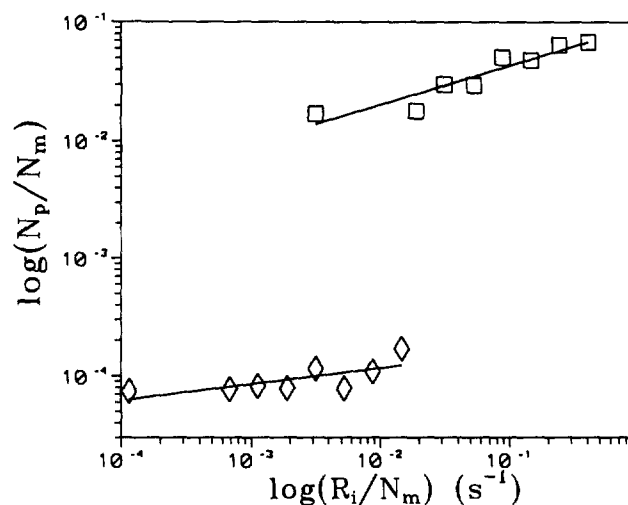


Figure 8 Fraction of micelles that is ultimately converted to the latex particles as a function of the number of free radicals captured by one micelle. [NP-40] (wt%): □, 0; ◇, 100

equation provided that the monomer effect is not important.

$$M_m = ([S] - \text{CMS}(80^\circ\text{C}))/m \quad (3)$$

where m is the number of surfactant molecules present in a micelle (i.e., aggregation number). The number of free radicals captured by one micelle is therefore equal to R_i/N_m , where $R_i = 2fK_d[I]$ is the generation rate of free radicals in the aqueous phase, f is the initiation efficiency factor, and K_d is the initiator decomposition rate constant. The kinetic parameters used in the calculation of N_p/N_m and R_i/N_m are listed in Table 2, and the results are shown in Figure 8. The parameter N_p/N_m represents the fraction of micelles that is ultimately converted to the latex particles. Theoretical analysis on the experiments with [NP-40] = 50 and 80 wt% was not conducted because the information about the mixed micelles (e.g., the structure, composition, and m of the mixed micelles) required for calculation is not available at this point of time. Figure 8 shows that N_p/N_m increases with increasing R_i/N_m and the slope of the $\log(N_p/N_m)$ versus $\log(R_i/N_m)$ data is 0.329 for the system stabilised only by SDS. A similar trend is observed for the reaction stabilised only by NP-40, but the rate of change in $\log(N_p/N_m)$ with $\log(R_i/N_m)$ is smaller (slope = 0.136). Furthermore, at constant R_i/N_m , the value of N_p/N_m for the system stabilised only by SDS is approximately two orders of magnitude greater than that for the system stabilised only by NP-40 (see the N_p/N_m data with R_i/N_m in the range of 10^{-3} – 10^{-2} s^{-1} in Figure 8). This result is consistent with our previous work and it implies that not all the nucleated primary particles can survive limited flocculation when NP-40 is used as the sole stabiliser¹².

So far, it has been shown that conventional Smith–Ewart case II theory ($n_s = 0.6$ and $n_i = 0.4$ in equation (1)) is only applicable to the STY emulsion polymerisation stabilised only by SDS. Incorporation of 50 wt% or more NP-40 into the surfactant mixture leads to dramatic deviations from Smith–Ewart case II theory. The parameters N_p and R_p for the NP-40 stabilised polymerisation system are relatively insensitive to changes in [I]. Furthermore, in terms of coagulum formation, the latex particles stabilised only by SDS or NP-40 are quite stable during the course of polymerisation. For the system with [NP-40] = 50 or 80 wt%, the transition from a stable to an unstable colloidal state occurs at [I] = 6.4×10^{-3} – 1.1×10^{-2} M, judging from the experimental data of N_p , R_p and total scrap. This result suggests that the parameters [NP-40] and [I] should play an important role in controlling the latex stability during polymerisation. This transitional behaviour will be discussed in detail in the following section.

Stability of latex particles during polymerisation

The shear force generated by intensive agitation may cause significant turbulence in a stirred-tank reactor, which increases both the force and frequency of collisions among the interactive latex particles. Thus, these latex particles under mechanical agitation may coagulate with one another due to the attractive van der Waals force during polymerisation. It is postulated that the total scrap formed during polymerisation is determined by the fraction of the particle surface covered by NP-40 (θ) and the ratio of the thickness of the NP-40 adsorption layer (δ) to the thickness of the electric double layer (κ^{-1}) around the latex particles $\kappa\delta$ ($\delta/\kappa^{-1} = \kappa\delta$)^{22–25}. The electric double layer around these latex particles originates from the adsorbed SDS species and the sulfate groups (SO_4^-) on the particle surface derived from the persulfate initiator. According to De Witt and van de Ven²³, the parameter θ and the ratio $\kappa\delta$ may play an important role in the bridging flocculation process. At lower values of $\kappa\delta$ (i.e., $\delta < \kappa^{-1}$) the electrostatic repulsion force predominates the interparticle interaction process, leading to a relatively stable colloidal system. The colloidal system becomes unstable due to bridging flocculation when the ratio $\kappa\delta$ is equal to unity. Under the condition of $\theta \rightarrow 1$ and $\kappa\delta > 1$ (i.e., $\delta \gg \kappa^{-1}$), the colloidal system is stable as a result of steric stabilisation.

As shown in Figures 4 and 5, the total scrap data for the system with [NP-40] = 0 wt% are quite low and they are insensitive to changes in [I]. The relatively low levels of total scrap are attributed to the extremely small ratio $\kappa\delta$ (i.e. $\delta \rightarrow 0$ and $\kappa\delta < 1$). This is because the good stability of the latex particles stabilised only by SDS during polymerisation is achieved mainly by electrostatic stabilisation. Similarly, the total scrap data for the system with [NP-40] = 100 wt% are quite low and, again, they are independent of [I]. In this case, the relatively low total scrap data are most likely due to the condition that the latex particles are well protected by NP-40 (i.e., $\theta \rightarrow 1$) and $\kappa\delta > 1$ (i.e., $\delta \gg \kappa^{-1}$). As a result of the predominant steric stabilisation mechanism, the polymer colloid shows an excellent stability in the course of polymerisation.

The total scrap data are strongly dependent on [I] for the system with [NP-40] = 50 or 80 wt% (see the circular or triangular data points in Figure 5). Increasing [I] will enhance the ionic strength of the aqueous solution. The increased ionic strength will compress the electric double layer around the latex particles and, hence, greatly reduce the thickness of the electric double layer (κ^{-1}). At constant

[S] (6×10^{-3} M) and [NP-40] (50 or 80 wt%), the parameter δ should not change very much during polymerisation. This may thus cause the ratio $\kappa\delta$ to approach unity and, thereby, reduce the colloidal stability significantly. On the other hand, increasing [I] may also result in an increase in the particle surface SO_4^- end-groups when the oligomeric radicals enter the monomer-swollen latex particles and polymerise therein. This will enhance the particle surface charge density and, thus, increase the thickness of the electric double layer κ^{-1} (or decrease κ). In this case, the ratio $\kappa\delta$ decreases to a value far below unity and, consequently, these latex particles can be stably dispersed in the aqueous phase during polymerisation.

When [I] is within the range of 1.4×10^{-3} – 6.5×10^{-3} M, the stabilising effect provided by the increased electric double layer thickness may counteract the destabilising effect caused by the increased ionic strength. At relatively low levels of [I], the system with [NP-40] = 50 or 80 wt% may thus produce relatively clean latex products. On the other hand, the destabilising effect may override the stabilising effect when [I] increases from 6.5×10^{-3} M to about 1.8×10^{-2} M. This will then cause the ratio $\kappa\delta$ to approach unity and greatly reduce the stability of latex particles during polymerisation. Thus, the higher the level of [I], the greater is the amount of coagulum formed during polymerisation. Beyond the maximal point occurring at [I] $\sim 1.8 \times 10^{-2}$ M, the total scrap decreases rapidly with increasing [I]. This is simply because the stabilising effect provided by the increased electric double layer thickness becomes predominant again. This may further increase the ratio $\kappa\delta$ and cause the coagulation process to cease when the ratio $\kappa\delta$ is greater than unity.

Although bridging flocculation has not been reported in the literature for the molecular weight range of the hydrophilic part of NP-40 (40 units of ethylene oxide ~ 2000 g mol⁻¹), the proposed bridging flocculation mechanism may provide qualitative explanations for the total scrap *versus* [I] data presented in this work. It is postulated that the hydrophobic nonylphenol group of NP-40 will be anchored firmly on the latex particle surface. This may result in an extended conformation in water for the ethylene oxide chain of NP-40 and, thereby, increase the probability of bridging flocculation between two approaching latex particles. According to Chu and Cheng²⁶, the thickness of the NP-40 adsorption layer around the latex particles (δ) is 7.3 nm, which is comparable to the value of δ reported for the flocculated polystyrene latex particles induced by poly(ethylene oxide)²³. This provides supporting evidence of significant bridging flocculation occurring during the reaction for the system with [NP-40] = 50 or 80 wt%. Furthermore, the shear force generated by intensive agitation may bring the latex particles into close contact and, thereby, increase the probability of bridging flocculation. However, further research is required to verify the bridging flocculation mechanism proposed in this work.

Another possible explanation for the total scrap *versus* [I] data for the polymerisation systems with [NP-40] = 50 or 80 wt% is that the ethylene oxide unit of NP-40 can form a complex structure with the SO_4^- end-group (derived from the persulfate initiator) on the neighbouring latex particle surface²⁷. This complex formation mechanism may thus cause the interactive particles to coagulate with one another during polymerisation. When [I] is below 6.5×10^{-3} M, the ionic strength of the aqueous solution is not strong enough to significantly compress the electric double layer around the latex particles. As a result, the synergetic stabilisation

Table 3 Effect of total concentration of sodium ions on the amount of coagulum formed during polymerisation: $[S] = 6 \times 10^{-3}$ M and $[NP-40] = 50$ wt%

$[I] \times 10^{-3}$ (M)	$[Na_2SO_4] \times 10^{-3}$ (M) ^a	$[Na^+] \times 10^{-3}$ (M)	d_p (nm)	$N_p \times 10^{17}$ (1/L)	$R_p \times 10^{-4}$ (M s ⁻¹)	\bar{n}	Total scrap (%)
17.70	–	35.40	95	2.65	9.47	1.21	28.31
2.31	15.40	35.40	122	1.69	5.04	1.01	26.47
2.31	–	4.62	84	5.40	13.10	0.82	2.53

^aConcentration of sodium sulfate

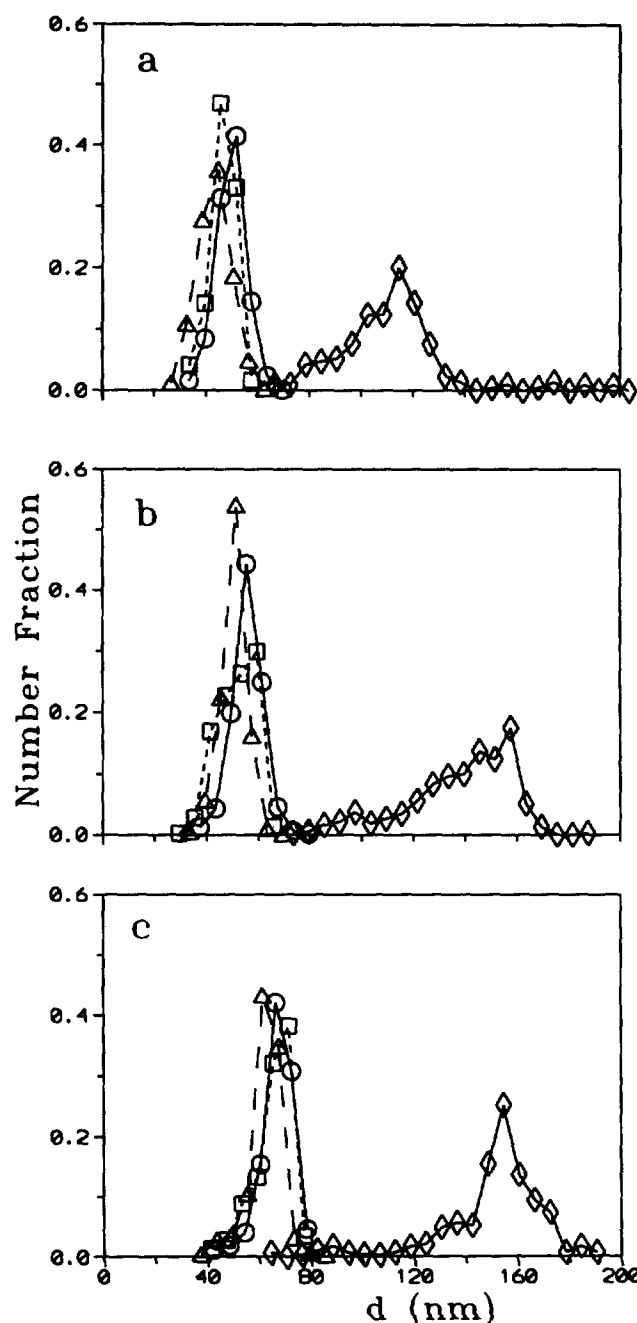
effects provided by the mixed SDS/NP-40 surfactants make the colloidal system rather stable during polymerisation. On the other hand, the electrostatic repulsion force between two approaching particles is greatly reduced due to the increased ionic strength with increasing $[I]$ ($6.5 \times 10^{-3} \rightarrow 1.8 \times 10^{-2}$ M). This may promote the complex formation process and result in an increase in the total scrap with $[I]$. Further increasing $[I]$, the extremely high concentration of counterion Na^+ ($[Na^+]$) in the aqueous phase may lower the electrostatic force exerted by the particle surface SO_4^- end-groups and, thereby, reduce the degree of complex formation significantly. This screening effect may thus result in polymer colloids with relatively low levels of coagulum.

It has been shown that the influence of $[Na^+]$ on the amount of coagulum produced during polymerisation is significant for the system with $[NP-40] = 50$ or 80 wt%. One experiment with constant $[Na^+]$ ($2(2.31 \times 10^{-3} + 1.54 \times 10^{-2}) = 3.54 \times 10^{-2}$ M) achieved by using 2.31×10^{-3} M $Na_2S_2O_8$ and 1.54×10^{-2} M Na_2SO_4 (a non-reactive salt) was carried out to verify this argument. The parameters $[S]$ and $[NP-40]$ were kept constant at 6×10^{-3} M and 50 wt%, respectively, in this experiment. Some of the experimental results are listed in Table 3. As expected, the system with the same $[Na^+]$ (3.54×10^{-2} M) results in comparable total scrap data (ca. 27%), even though the levels of initiator are quite different (2.31×10^{-3} versus 1.77×10^{-2} M). For comparison, the system with $[S]$, $[NP-40]$, $[I]$ and $[Na^+]$ equal to 6×10^{-3} M, 50 wt%, 2.31×10^{-3} M, and 4.62×10^{-3} M, respectively, was also included in Table 3. At constant $[I]$, the total scrap is greatly reduced when $[Na^+]$ decreases from 3.54×10^{-2} to 4.62×10^{-3} M. These experimental data further support the bridging flocculation mechanism discussed above.

Latex particle size and particle size distribution

For the systems with various levels of $[NP-40]$ (0, 50, 80 and 100 wt%), the latex samples taken at low (ca. 23%, at the early stage of Interval II), intermediate (ca. 50%, at the early state of Interval III) and high (ca. 95%, at the end of polymerisation) levels of monomer conversion X were further examined by TEM to study the particle nucleation and growth mechanisms. The parameter $[I]$ was kept constant at 1.38×10^{-3} M in this series of experiments. The particle size distribution data are shown in Figure 9. Representative TEM photographs for the systems with $[NP-40] = 0$ and 100 wt% are shown in Figure 10. Some of the numeric data are also summarised in Table 4. The symbols d_n , d_w , PDI and σ represent the number averaged particle size, weight averaged particle size, polydispersity index defined as d_w/d_n and standard deviation, respectively, for the 'dried' particles.

Figure 9 shows that the systems with $[NP-40] = 0, 50$ and 80 wt% result in comparable latex particle sizes and relatively monodisperse size distributions throughout the reaction. On the other hand, the system stabilised only by NP-40 exhibits the largest particle size and the broadest size


Figure 9 Particle size distribution data for the latex samples taken at (a) low (ca. 23%), (b) intermediate (ca. 50%), and (c) high (ca. 95%) levels of monomer conversion. $[NP-40]$ (wt%): \square , 0; \circ , 50; \triangle , 80; \diamond , 100

distribution, which may be attributed to the longer particle nucleation period. The long tail shifting toward smaller particle sizes (see Figure 9) and the slightly larger PDI data (see Table 4) further serve as supporting evidence for the longer particle nucleation period. Another possible explanation for the unique particle nucleation and growth behaviour

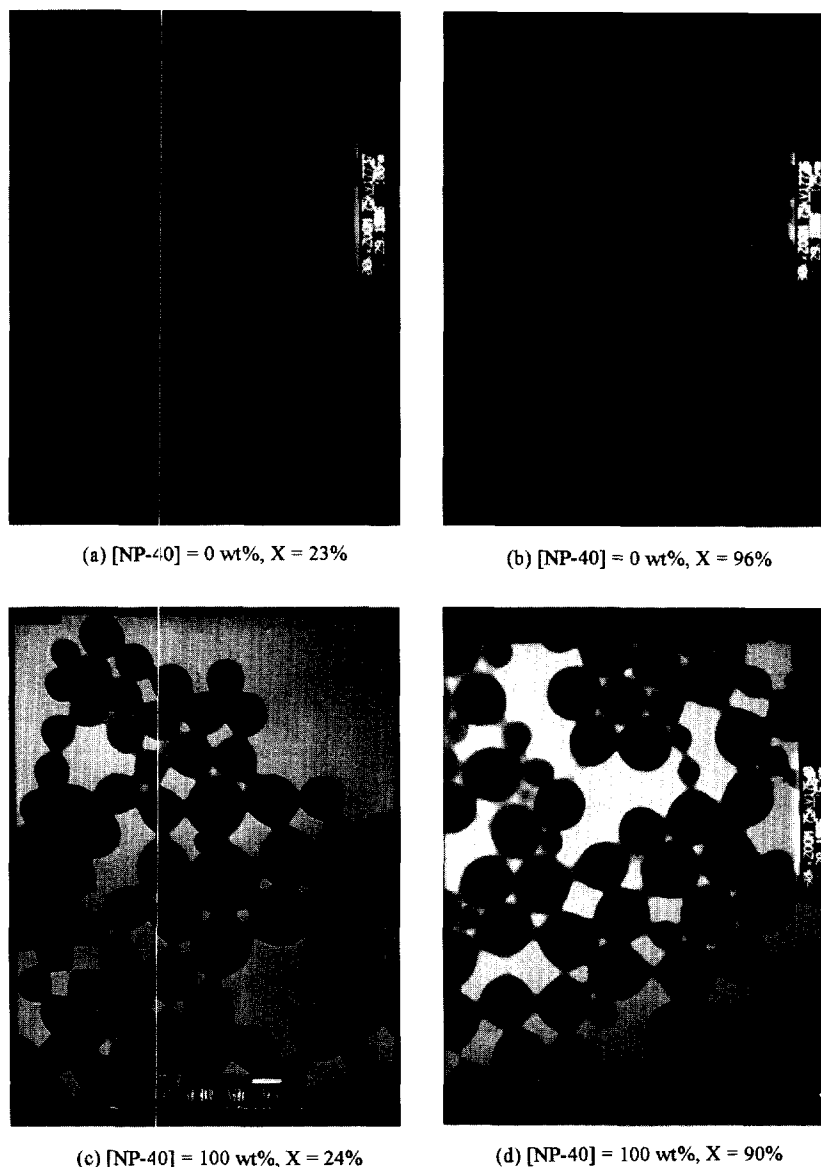


Figure 10 Representative TEM photographs for the latex samples taken at low and high levels of monomer conversion: (a) [NP-40] = 0 wt% at $X = 23\%$; (b) [NP-40] = 0 wt% at $X = 93\%$; (c) [NP-40] = 100 wt% at $X = 24\%$; (d) [NP-40] = 100 wt% at $X = 90\%$

Table 4 Particle size and particle size distribution data determined by TEM for the latex samples with various levels of [NP-40]: [S] = 6×10^{-3} M and [I] = 1.38×10^{-3} M

[NP-40] (wt%)	X (%)	d_w (nm)	d_n (nm)	PDI ^a	σ (nm) ^b
0	22.9	47.9	46.3	1.03	4.5
	50.9	54.9	51.6	1.06	7.0
	97.5	68.8	67.3	1.02	5.6
50	22.3	51.8	49.5	1.05	5.6
	45.0	57.9	55.5	1.04	5.8
	93.8	68.6	66.7	1.03	6.2
80	24.4	46.6	43.1	1.08	6.4
	48.2	52.0	50.4	1.03	4.7
	98.9	64.3	62.1	1.04	6.3
100	23.8	132.4	111.5	1.19	21.1
	54.4	146.9	137.6	1.07	20.3
	90.0	157.6	149.7	1.05	20.4

^aPolydispersity index = d_w/d_n

^bStandard deviation

associated with the system with [NP-40] = 100 wt% is that the nonionic surfactant with a concentration of 6×10^{-3} M is not high enough to prohibit the growing latex particles from flocculating with one another¹². This limited flocculation

may also contribute to the broader size distribution. On the other hand, the mixed surfactant system (SDS/NP-40) containing 20 wt% SDS or more can be very effective for stabilising these latex particles during the particle nucleation period. This makes the polymerisation system with [NP-40] = 0, 50 and 80 wt% exhibit very different particle nucleation and growth behaviour from the system with NP-40 as the sole stabiliser. In addition, the size distribution becomes narrower as polymerisation proceeds (see the decreased PDI data with increasing X in Table 4), which is typical of the relatively long residence time in a batch reactor.

CONCLUSIONS

The influence of the persulfate initiator on the batch emulsion polymerisation of STY stabilised by the mixed SDS/NP-40 surfactants was investigated in this work. The parameter [I] was varied from 5.02×10^{-4} to 9.20×10^{-2} M. The polymerisation system stabilised only by SDS ([NP-40] = 0 wt%) results in an increase in R_p with [I]. For the system with NP-40 as the sole stabiliser ([NP-40] =

100 wt%), R_p remains relatively constant when [I] increases. As to the system with [NP-40] = 50 or 80 wt%, R_p first increases to a maximum at [I] $\sim 6.4 \times 10^{-3}$ M and thereafter starts to decrease with increasing [I]. The greater the number of reaction loci (N_p), the faster the rate of polymerisation (R_p). The slower rate of polymerisation for the system stabilised only by NP-40 is due to the smaller value of N_p and/or the more intensive limited flocculation occurring during the particle growth period.

Conventional Smith–Ewart case II theory (i.e., $n_s = 0.6$ and $n_i = 0.4$ in the relationship $N_p \sim [S]^{n_s} [I]^{n_i}$) is only applicable to the STY emulsion polymerisation stabilised only by SDS. On the other hand, incorporation of 50 wt% or more NP-40 into the surfactant mixture leads to deviations from Smith–Ewart case II theory. The parameter n_i first increases to a maximum and then decreases with an increase in [NP-40]. The parameters N_p and R_p for the system with [NP-40] = 100 wt% are relatively insensitive to changes in [I]. The latex particles stabilised only by SDS or NP-40 are quite stable in the course of polymerisation. For the system with [NP-40] = 50 or 80 wt%, transition from a stable to an unstable colloidal state occurs at [I] = 6.4×10^{-3} – 1.1×10^{-2} M. Furthermore, the total scrap, presumably caused by the bridging flocculation mechanism, first remains relatively constant and then increases rapidly to a maximum when [I] increases. Beyond the maximal point, the amount of coagulum starts to decrease with increasing [I]. The fraction of the particle surface covered by NP-40 (θ) and the ratio of the thickness of the NP-40 adsorption layer to the thickness of the electric double layer around the latex particles ($\kappa\delta$) were postulated to be the crucial parameters in determining colloidal stability during the reaction. Another postulation proposed for the total scrap versus [I] data associated with the system with [NP-40] = 50 or 80 wt% is related to the complex formation between the ethylene oxide unit of NP-40 and the particle surface SO_4^- end-group derived from the persulfate initiator.

At constant [I] (1.38×10^{-3} M), the systems with [NP-40] = 0, 50 and 80 wt% result in comparable latex particle sizes and relatively monodisperse size distributions throughout the reaction. On the other hand, the system with [NP-40] = 100 wt% shows the largest particle size and the broadest size distribution, which may be attributed to the long particle nucleation period and/or limited flocculation. Incorporation of a small amount of SDS (20 wt% or more) into the system makes it stable enough to withstand limited flocculation and hence results in quite different particle size and size distribution data from those for the latex particles stabilised only by NP-40.

ACKNOWLEDGEMENTS

This work was supported by the National Science Council of Taiwan, Republic of China. The authors would like to thank J. S. Lee for performing part of the experiments.

REFERENCES

1. Verwey, E. J. W. and Overbeek, J. Th. G., *Theory of the Stability of Lyophobic Colloids*. Elsevier, New York, 1943.
2. Napper, D. H., *Polymeric Stabilization of Colloidal Dispersions*. Academic Press, London, 1983.
3. Chern, C. S. and Hsu, H., *Journal of Applied Polymer Science*, 1995, **55**, 571.
4. Chern, C. S. and Lin, F. Y., *Journal of Macromolecular Science—Pure Applied Chemistry*, 1996, **A33**, 1077.
5. Ottewill, R. H., Satgurunathan, R., Waite, F. A. and Westby, J. M., *British Polymer Journal*, 1987, **19**, 435.
6. Ottewill, R. H. and Satgurunathan, R., *Colloid and Polymer Science*, 1995, **273**, 379.
7. Harkins, W. D., *Journal of American Chemical Society*, 1947, **69**, 1428.
8. Smith, W. V. and Ewart, R. W., *Journal of Chemical Physics*, 1948, **16**, 592.
9. Smith, W. V., *Journal of the American Chemical Society*, 1948, **70**, 3695.
10. Smith, W. V., *Journal of the American Chemical Society*, 1949, **71**, 4077.
11. Chen, L. J., Lin, S. Y., Chern, C. S. and Wu, S. C., *Colloid Surf. A*, 1997, **122**, 161.
12. Chern, C. S., Lin, S. Y., Chen, L. J. and Wu, S. C., *Polymer*, 1997, **38**, 1977.
13. Matheson, M. S., Auer, E. E., Bevilacqua, E. B. and Hart, E. J., *Journal of the American Chemical Society*, 1949, **71**, 497.
14. Odian, G., *Principles of Polymerization*. Wiley, New York, 1981.
15. Bartholome, E., Gerrens, H., Herbeck, R. and Weitz, H. M., *Zeitschrift für Elektrochemie*, 1956, **60**, 334.
16. Chu, H. and Piirma, I., *Polymer Bulletin*, 1989, **21**, 301.
17. Unzueta, E. and Forcada, J., *Polymer*, 1995, **36**, 1045.
18. Kolthoff, I. M. and Miller, I. K., *Journal of the American Chemical Society*, 1951, **73**, 3055.
19. Tartar, H. V., *Journal of Physical Chemistry*, 1955, **59**, 1195.
20. Venable, R. L. and Nauman, R. V., *Journal of Physical Chemistry*, 1964, **68**, 3498.
21. Becher, P., *Journal of Colloid Science*, 1961, **16**, 49.
22. Pelssers, E. G.M., Cohen Sturat, M. A. and Fleer, G. J., *Journal of the Chemical Society, Faraday Transactions*, 1990, **86**, 1355.
23. De Witt, J. A. and van de Ven, T. G.M., *Advances in Colloid and Interface Science*, 1992, **42**, 41.
24. Chern, C. S., Shi, Y. L. and Wu, J. S., *Polymer International*, 1996, **40**, 129.
25. Chern, C. S., Liou, Y. C. and Tsai, W. Y., *Journal of Macromolecular Science—Pure Applied Chemistry*, 1996, **A33**, 1063.
26. Chu, H. H. and Cheng, H. C., *IUPAC International Symposium, Functional and High Performance Polymers*, Taipei, Taiwan, 14–16 November 1994. Preprints, p. 413 (paper no. 6-E-13).
27. Mura, J. L. and Riess, G., *Polymer Advanced Techniques*, 1995, **6**, 497.